L.M. Vikhor, V.Ya. Mykhailovsky, V.R. Bilinsky-Slotylo

Institute of Thermoelectricity NAS and MES of Ukraine,
1, Nauky Str., Chernivtsi, 58029, Ukraine

SEGMENTED AND MULTI-STAGE STRUCTURES BASED ON *PbTe/Zn$_4$Sb$_3$* FOR THERMOELECTRIC GENERATOR MODULES

This paper presents the results of designing segmented thermoelectric modules, as well as functionally graded material (FGM)-based modules and multi-stage structures of PbTe/Zn$_4$Sb$_3$-based materials for use in thermoelectric power converters with the hot side temperature level 780 K.
Key words: generator modules, heat recovery, power converters.

Introduction

Among thermoelectric materials used for creation of generator modules for the hot side temperature level 775-875K, *PbTe* is traditionally employed [1]. At current stage of development of science and technology, the presence of lead and tellurium in this material is not a limiting factor for its mass use, in particular, for the recovery of waste heat from vehicles, industry, etc. However, unlike *n-PbTe*, *p*-type has a low mechanical strength and unstable parameters, especially at elevated temperatures [2]. Most frequently an alternative to *p-PbTe* is *GeTe-AgSbTe* [3-5], however, taking into account the world reserves and the cost of source elements listed in Table 1 [6], the use of *Ag*, *Ge* and *Te* as the basic components for creation of thermoelectric power converters should be restricted.

Table 1

The cost, production outputs and world reserves of components used for creation of medium-temperature thermoelectric materials [6]

Material / Characteristics	Pb	Te	Ag	Ge	Sb	Zn
Price (2011), \$/kg	2.73	360	1109	1400	15.1	2.34
Production (2011),1000 t	4.5	0.12	23.8	118	169	12.4
World reserves, 1000 t	85	24	530	> 500	1800	250

Within recent years a number of researchers have obtained a series of thermoelectric materials with potentially high operating characteristics [7-10]. Among them, good promise is shown by β-*Zn$_4$Sb$_3$* that has a high figure of merit (*ZT* = 1.2 – 1.4 at 675 K) with a rather low prime cost. The above factors prove the possibility of using β-*Zn$_4$Sb$_3$* material as a *p*-type leg for medium-temperature thermoelectric modules.

The purpose of this work is to design and evaluate the efficiency of segmented, multi-stage and FGM modules based on *PbTe/Zn$_4$Sb$_3$*, as well as to optimize such structures for achieving maximum module efficiency.

Design of segmented thermoelectric modules and FGM modules

Calculation and design of modules was done with the use of optimal control theory methods [11] and experimentally measured concentration-temperature dependences of α, σ, κ parameters of *n*-type *PbTe* samples doped with iodine [12] and europium [13], as well as *p*-type samples of $Zn_{3.96+x}Cd_{0.04}Sb_3$ [14] and $(Zn_{1-x}Cd_x)_4Sb_3$ [15]. Such dependences for the best samples with different doping level, different composition and, respectively, different current carrier concentration are given in Figs. 1 and 2.
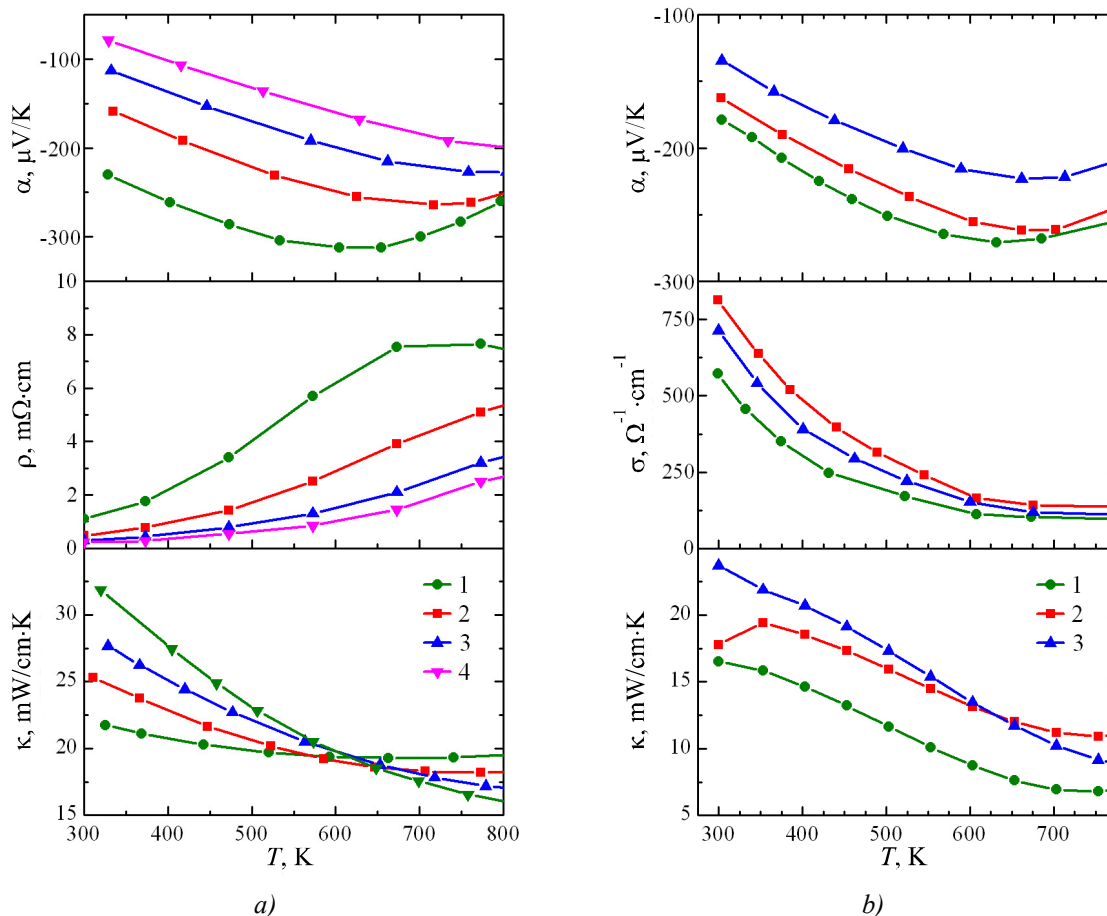

a)   *b)*

Fig. 1. Temperature dependences of thermoelectric parameters of PbTe-based n-type materials:
a) PbTe+x mol.% PbI₂ (1 − x = 0.01; 2 − x = 0.03; 3 − x = 0.055; 4 − x = 0.1) [12];
b) PbTe+x % Eu (1 − x = 1; 2 − x = 2; 3 − x = 3) [13].

The temperature dependences shown in Figs.1 and 2 were approximated by two-dimensional polynomials in the form of $\alpha^{n,p} = \alpha^{n,p}(\sigma_0^{n,p}, T)$, $\sigma^{n,p} = \sigma^{n,p}(\sigma_0^{n,p}, T)$, $\kappa^{n,p} = \kappa^{n,p}(\sigma_0^{n,p}, T)$. Polynomial coefficients were introduced into computer program as input data for the design of thermoelectric modules. Designations of module legs of such materials are given in Table 2.

Calculated in maximum efficiency mode, optimal energy characteristics (current *I*, voltage *U*, power *P*, efficiency η) of one- and two-segment modules, as well as FGM modules comprising 32 thermoelements (the height of legs 5.6 mm, the cross-sectional area of legs 4×4 mm²) are given in Table 3. The values of contact resistances in the calculations were assumed to be equal to $5 \cdot 10^{-5}$ $\Omega \cdot$cm². Optimization was performed by determination of such impurity concentrations in each segment material whereby thermoelement efficiency reaches a maximum with regard to optimal current densities in its legs and the height of segments.
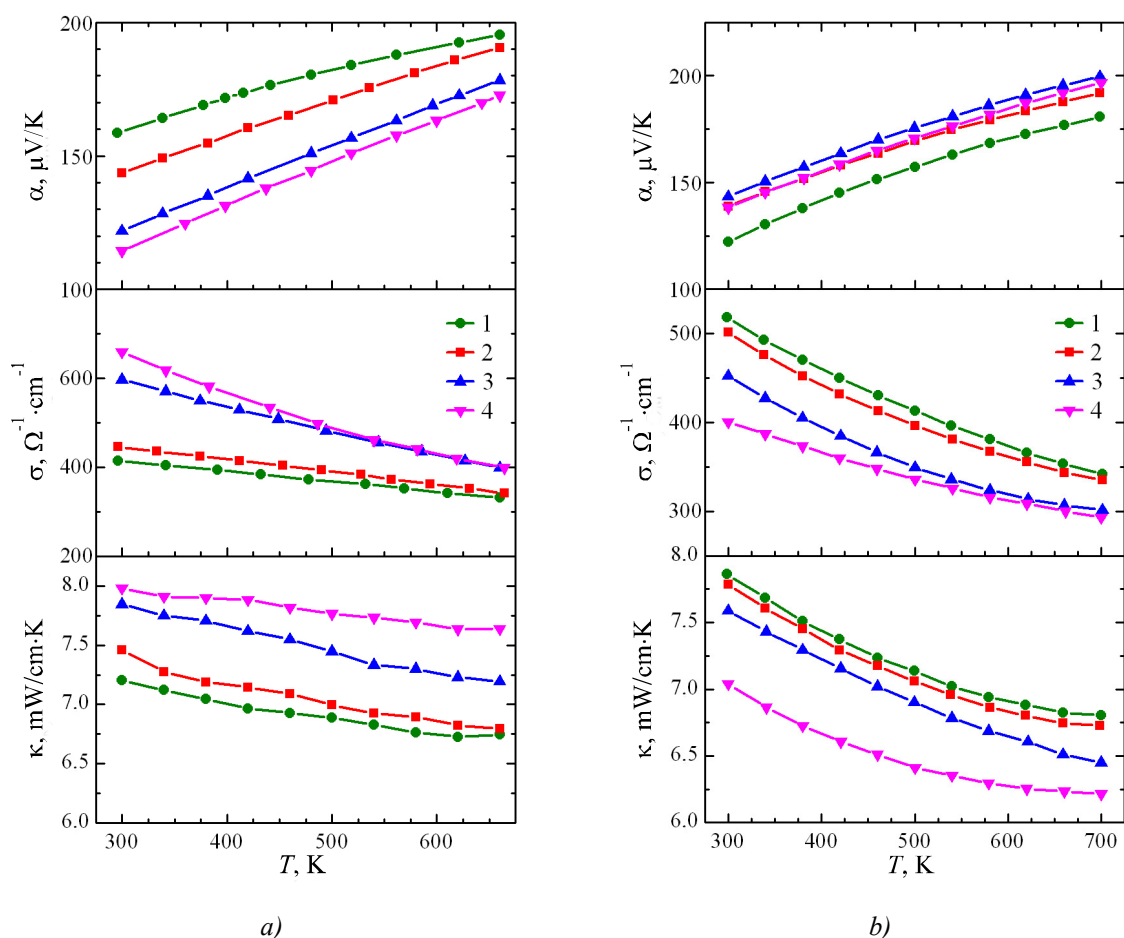
a)   *b)*

Fig. 2. Temperature dependences of thermoelectric parameters of Zn-Sb-based p-type materials:
a) $Zn_{3.96+x}Cd_{0.04}Sb_3$ (1 – x = –0.05; 2 – x = 0; 3 – x = 0.05; 4 – x = 0.1) [14];
b) $(Zn_{1-x}Cd_x)_4Sb_3$ (1 – x = 0; 2 – x = 0.005; 3 – x = 0.01; 4 – x = 0.015) [15].

Table 2

Leg designations of generator modules of PbTe/Zn₄Sb₃-based thermoelectric materials

Designation	*n*-type leg	Designation	*p*-type leg
S1	$PbTe<x$ mol.% $PbI_2>$ $(x = 0.01 – 0.1)$ [12]	S2	$Zn_{3.96+x}Cd_{0.04}Sb_3$ $(x = –0.05 – 0.1)$ [14]
S3	$PbTe<x$ % $Eu>$ $(x = 1 – 3)$ [13]	S4	$(Zn_{1-x}Cd_x)_4Sb_3$ $(x = 0 – 0.015)$ [15]

Analysis of resulting data shows that one-segment modules S1-S2 and S1-S4 have commensurate efficiencies ($\eta \approx 7.5 – 7.6\%$). However, with transition to two segments, the efficiency of S1-S2 is $\eta = 14.65$ %, whereas the efficiency of module S1-S4 is considerably lower $\eta = 12.25$ %. Similar results were obtained for modules S3-S2 and S3-S4. With the use of europium-doped *PbTe* (S3) as *n*-type leg, the efficiency of one-segment modules is reduced ($\eta \approx 6$ %), and that of two-segment modules remains practically the same as in the case when iodine-doped lead telluride (S1) is selected as *n*-type leg.

<div align="right"><u>*Table 3*</u></div>

Characteristics of generator modules of PbTe/Zn₄Sb₃-based materials
for the operating temperature range of 323 – 773 K

Designation of modules			Optimal parameters of leg materials (segments)	l_{leg} (l_{segm}), mm	P, W	I, A	U, V	η, %
One-segment (S1-S2)	*n*-type leg		$x = 0.02$	5.6	11	3.35	3.28	7.6
	p-type leg		$x = 0.062$	5.6				
Two-segment (S1-S2)	*n*-type leg	cold	$x = 0.01$	3.2	25.8	7.62	3.39	14.65
		hot	$x = 0.064$	2.4				
	p-type leg	cold	$x = -0.048$	2.4				
		hot	$x = 0.09$	3.2				
FGM module (S1-S2)	*n*-type leg		Fig 3 *a*	5.6	23.5	7.34	3.2	15.52
	p-type leg			5.6				
One-segment (S1-S4)	*n*-type leg		$x = 0.019$	5.6	10.59	3.125	3.39	7.47
	p-type leg		$x = 0.004$	5.6				
Two-segment (S1-S4)	*n*-type leg	cold	$x = 0.01$	3.3	19.26	5.47	3.52	12.25
		hot	$x = 0.059$	2.3				
	p-type leg	cold	$x = 0.0045$	2.3				
		hot	$x = 0.0075$	3.3				
FGM module (S1-S4)	*n*-type leg		Fig 3 *b*	5.6	18.5	5.6	3.31	14.04
	p-type leg			5.6				
One-segment (S3-S2)	*n*-type leg		$x = 1.65$	5.6	5.43	1.64	3.32	6.2
	p-type leg		$x = -0.048$	5.6				
Two-segment (S3-S2)	*n*-type leg	cold	$x = 1.1$	2.3	17.04	5.49	3.1	14.5
		hot	$x = 2.8$	3.3				
	p-type leg	cold	$x = -0.03$	3.3				
		hot	$x = 0.03$	2.3				
FGM module (S3-S2)	*n*-type leg		Fig. 3 *c*	5.6	19	6.13	3.1	15.49
	p-type leg			5.6				
One-segment (S3-S4)	*n*-type leg		$x = 1.73$	5.6	5.47	1.72	3.18	6.01
	p-type leg		$x = 0.0063$	5.6				
Two-segment (S3-S4)	*n*-type leg	cold	$x = 1.2$	2	14.3	4.5	3.17	12.67
		hot	$x = 2.43$	3.6				
	p-type leg	cold	$x = 0.006$	3.6				
		hot	$x = 0.0129$	2				
FGM module (S3-S4)	*n*-type leg		Fig. 3 *d*	5.6	15	4.84	3.1	13.88
	p-type leg			5.6				

Hence, in the selection of n-leg material, preference should be given to iodine-doped *PbTe* (S1), and p-leg material – $Zn_{3.96+x}Cd_{0.04}Sb_3$ (S2). Using materials with a certain impurity concentration distribution along the height of legs (Fig. 3), one can obtain modules characterized by higher efficiency values than their two-segment analogs (Table 3).
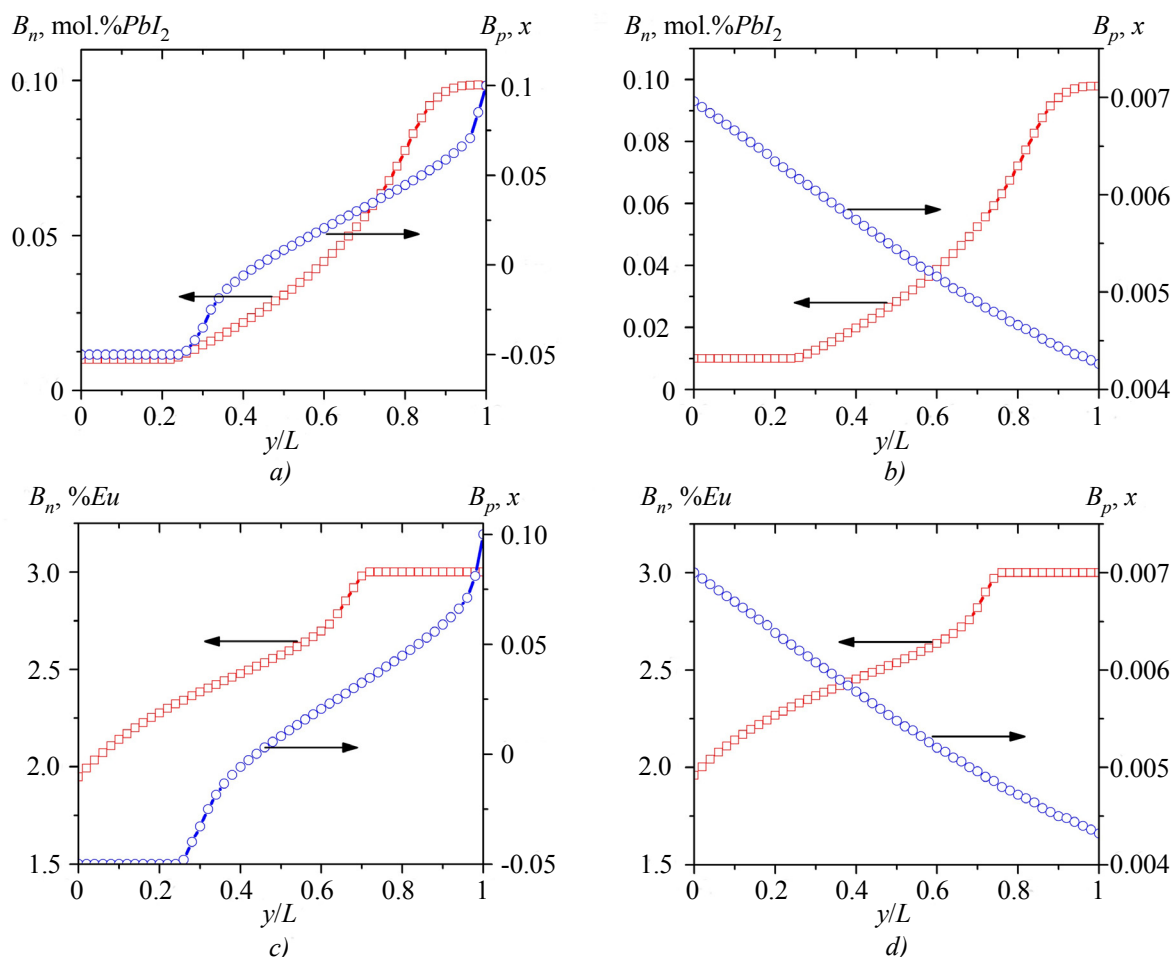

Fig. 3. Distribution of impurity content (composition) in FGM legs
for generator modules: a) S1-S2; b) S1-S4;
c) S3-S2; d) S3-S4.

Comparison of investigated segmented structures based on *PbTe/Zn₄Sb₃* to modules based on n- and p-*PbTe* [16] shows that their efficiencies are commensurate, and the main advantage of β-*Zn₄Sb₃* is its considerably lower cost and superior mechanical properties.

Multi-stage generator modules of *PbTe/Zn₄Sb₃*-based materials

The choice of leg materials for each module stage was done using optimal control theory methods [11], so that the cold and hot stages be characterized by maximum efficiency in the temperature range of 323 – 523 K and 523 – 773 K, respectively. The input data for optimization were experimentally measured temperature dependences of thermoelectric parameters (α, σ and κ) of iodine-doped n-*PbTe* [12] and p-$Zn_{3.96+x}Cd_{0.04}Sb_3$ [14] materials with different doping degrees (Fig. 1 *a*, 2 *a*), which showed the best results for the segmented modules. Optimal materials for two-stage module legs are listed in Table 4.

Using the optimal materials for *n*- and *p*-type legs, calculations of two-stage module structures were made (Table 5) with a series connection of the cold and hot stages, as well as thermal and electric matching of stages. The heat-absorbing and heat-releasing surfaces of modules are identical and make 40×40 mm^2.

Table 4

Optimal materials for a two-stage module

Designation of stages and legs		Leg material	Optimal concentration
cold	*n*-type	*PbTe*+*x* mol.% *PbI$_2$*	*x* = 0.01
	p-type	*Zn$_{3.96+x}$Cd$_{0.04}$Sb$_3$*	*x* = −0.048
hot	*n*-type	*PbTe*+*x* mol.% *PbI$_2$*	*x* = 0.059
	p-type	*Zn$_{3.96+x}$Cd$_{0.04}$Sb$_3$*	*x* = 0.09

From the data listed in Table 5 it is seen that with the increase in the dimensions of two-stage module thermoelements, a better efficiency is achieved with a considerably lower electric power (module № 1). To create a two-stage module with a maximum power for given operating temperature level, preference should be given to structure of module № 3. In so doing, the amount of thermoelectric material necessary for creation of a module is 1.5 times smaller compared to module № 2 and a factor of 3.6 smaller compared to module № 1.

Table 5

Calculated parameters of two-stage generator modules
of PbTe/Zn$_4$Sb$_3$-based materials at T_h = 773 K, T_c = 323 K

№	Parameter	Parameter value		
		Module №1	Module №2	Module №3
1.	Cross-sectional area of the cold and hot stage legs, mm^2	4×4	1.8×4.3	1.5×1.5
2.	Cold stage leg height, mm	5.1	2.9	1.8
3.	Hot stage leg height, mm	5.8	3.2	2
4.	Number of leg couples of the cold and hot stages	32	48	160
5.	Electric power, *P*, W	7.62	9.78	14.79
6.	Voltage *U*, V	2.75	4.1	6.7
7.	Current *I*, A	2.77	2.38	2.2
8.	Efficiency η, %	13.18	13.07	12.91
9.	Amount of thermoelectric material, cm^3	5.58	2.27	1.52

Dependences of efficiency and electric power of two-stage modules on the hot side temperature are given in Fig. 4.
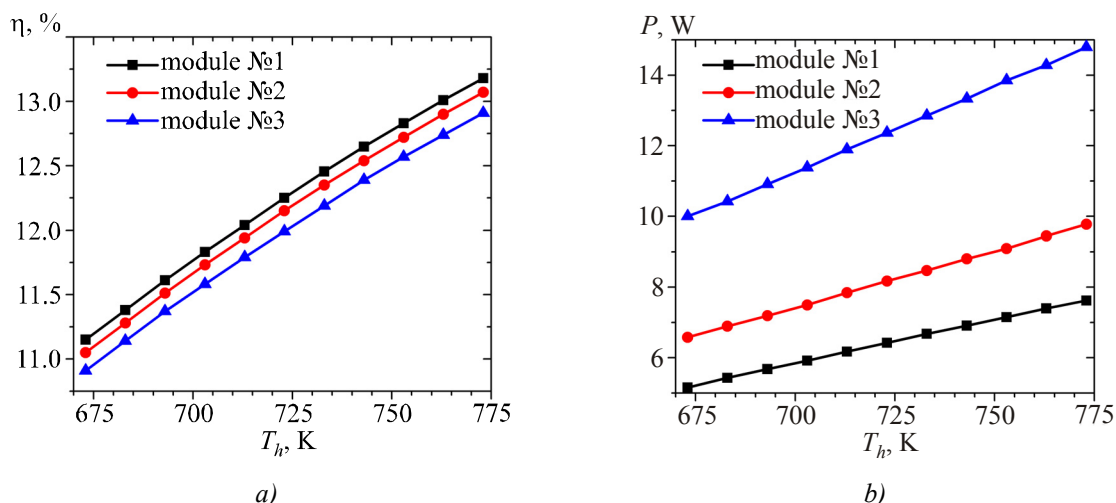
Fig. 4. Dependences of efficiency (a) and electric power (b) of two-stage modules based on PbTe/Zn₄Sb₃ on the hot side temperature at T_c = 323 K.

As is evident from Fig. 4, in the range of hot side temperatures 673 – 773 K dependences of efficiency on the hot side temperature for modules № 1 – 3 are similar, the efficiency is increased from ~ 11 to ~ 13 %, the electric power of module № 3 is much higher as compared to the other two structures (by a factor of ~ 2).

Conclusions

Using optimal control theory methods, design of segmented and multi-stage modules of *PbTe/Zn₄Sb₃* –based materials is performed. Optimal concentrations of doping impurities for leg materials and optimal geometric parameters of legs whereby maximum efficiency of thermoelectric generator modules is achieved in the temperature range of 323 – 773 K are determined.

It is shown that the efficiency of one-segment modules of *PbTe/Zn₄Sb₃* materials is $\eta \approx 6 – 7.5$ %, two-segment – $\eta \approx 12.5 – 14.5$ %, FGM modules – $\eta \approx 14 – 15.5$ %, and multi-stage structures – $\eta \approx 13$ %. Under defined geometric parameters of multi-stage modules the optimal interstage temperature is within 495 – 525 K.

Thermoelectric structures based on *n-PbTe/p-Zn₄Sb₃* and *n-PbTe/p-PbTe* are characterized by identical efficiency. However, as compared to *p-PbTe*, *p-Zn₄Sb₃* has essentially lower cost and better mechanical properties, which on the whole offers it the advantage in the choice of a medium-temperature thermoelectric material for generator modules.

References

1. Z.H. Dughaish, Lead Telluride as a Thermoelectric Material for Thermoelectric Power Generation, *Physica B* **322**, 205 (2002).

2. E.P. Sabo, Technology of Chalcogenide Thermoelements, Physical Fundamentals, Chapter 1, Structure and Properties of Materials, *J. Thermoelectricity* **3**, 29 – 41 (2000).

3. S.H. Yang, T.J. Zhu, S.N. Zhang, J.J. Shen, X.B. Zhao, Natural Microstructure and Thermoelectric Performance of (GeTe)₈₀(AgᵧSb₂₋ᵧTe₃₋ᵧ)₂₀, *J. Electronic Materials* **39** (9), 2127 (2010).

4. B.S. Kim, I.H. Kim, J.K. Lee, N.K. Min, M.W. Oh, S.D. Park, H.W. Lee, and M.H. Kim, Electron Transport Properties of Rapidly Solidified (GeTe)ₓ(AgSbTe₂)₁₋ₓ Pseudobinary Thermoelectric Compounds, *Electronic Materials Letters* **6** (4), 181 (2010).

5. E.A. Skrabek, D.S. Trimmer, Properties of the General TAGS System. *CRC Handbook of Thermoelectrics*, edited by D.M. Rowe, 1995, p. 267.

6. Mineral Commodity Summaries 2012, *U.S. Geological Survey* (Reston: Virginia, 2012), 198 p.

7. D.J.Singh, Electronic Transport in Old and New Thermoelectric Materials, *Science of Advanced Materials* **3**, 561 (2011).

8. J.-F. Li, W.-Sh. Liu, L.-D. Zhao, and M. Zhou, High-Performance Nanostructured Thermoelectric Materials, *NPG Asia Mater*. **2** (4), 152 (2010).

9. T.M. Tritt, Thermoelectric Phenomena, Materials, and Applications, *Annual Review of Materials Research* **41**, 433 (2011).

10. G.J. Snyder, E.S. Toberer, Complex Thermoelectric Materials, *Nature Materials* **7**, 105 (2008).

11. L.I. Anatychuk, L.N. Vikhor, *Thermoelectricity, Vol. IV, Functionally Graded Thermoelectric Materials* (Chernivtsi: Bukrek, 2012), 182 p.

12. V.M. Shperun, D.M. Freik, and R.I. Zapukhlyak, *Thermoelectricity of Lead Telluride and its Analogs* (Ivano-Frankivsk: Plai, 2000), 250 p.

13. H. Kong, Thermoelectric Property Studies on Lead Chalcogenides, *Double-Filled Cobalt Tri-Antimonide and Rare Earth-Ruthenium-Germanium, A Dissertation of Doctor of Philosophy (Physics),* The University of Michigan, 2008, 116 p.

14. Sh. Wang, F. Fu, X. She, G. Zheng, H. Li, X. Tang, Optimizing Thermoelectric Performance of *Cd*-Doped β-*Zn$_4$Sb$_3$* through Self-Adjusting Carrier Concentration, *Intermetallics* **19** (12), 1823 (2011).

15. Sh. Wang, H. Li, D. Qi, W. Xie, and X. Tang, Enhancement of the Thermoelectric Performance of β-*Zn$_4$Sb$_3$* by In Situ Nanostructures and Minute Cd-Doping, *Acta Materialia* **59**, 4805 (2011).

16. L.T. Strutynska, V.R. Bilinsky-Slotylo, V.Ya. Mykhaillovsky, Computer Design of Segmented *PbTe* Based Thermoelectric Modules, *J. Thermoelectricity* **3**, 44 – 49 (2012).